

Revealing the Surface and Subsurface Dynamics of the Sun's Polar Regions with Observations and 3D Radiative Hydrodynamic Modeling

Irina N. Kitiashvili(1), Wray A. Alan(1), Alexander G. Kosovichev(1,2), Junwei Zhao(3), J. Todd Hoeksema(3)

1) NASA Ames Research Center, 2) New Jersey Institute of Technology, 3) Stanford University

Abstract

The polar regions of the Sun are of great interest because of the correlation between the polar magnetic flux at a solar minimum and the strength of the following activity cycle. The current observational capabilities allow us to observe the polar regions only twice per year when the rotation axis of the Sun has a maximum inclination to the Earth's orbit. In this presentation, we discuss recent achievements in 3D radiative hydrodynamic simulations of the subsurface and surface dynamics in the high-latitude and polar regions, assuming the Carrington rotation rate and the rotation rates from helioseismic inferences and surface observations. We focus on analysis of latitudinal variations of a thin subsurface rotational shear layer – the leptocline. This analysis is being used for interpretation of observations from two NASA space missions, Hinode Solar Optical Telescope (SOT) and Solar Dynamics Observatory (SDO) Helioseismic and Magnetic Imager (HMI), to explore the coupling between subsurface and surface dynamics.

StellarBox Code

Numerical Model: Basic equations

The equations we solved are the grid-cell average conservation of mass:

$$\frac{\partial \rho}{\partial t} + (\rho u_i)_{,i} = 0$$

Conservation of momentum:

$$\frac{\partial \rho u_i}{\partial t} + \left(\rho u_i u_j + P_{ij}\right)_{,j} = -\rho \phi_{,i}$$

Conservation of energy:

$$\frac{\partial E}{\partial t} + \left(\begin{array}{l} E u_i + P_{ij} u_j - \kappa T_{,i} + \\ + \left(\frac{c}{4\pi}\right)^2 \frac{1}{\sigma} \left(B_{i,j} - B_{j,i}\right) B_j + F_i^{\mathrm{rad}} \end{array} \right)_{,i} = 0$$

Molecular and turbulent coefficients

with

$$P_{ij} = \left(p + \frac{2}{3}\mu u_{k,k} + \frac{1}{8\pi} B_k B_k \right) \delta_{ij} - \mu \left(u_{i,j} + u_{j,i}\right) - \frac{1}{4\pi} B_i B_j$$

Conservation of magnetic flux:

$$\frac{\partial B_i}{\partial t} + \left(u_j B_i - u_i B_j - \frac{c^2}{4\pi\sigma} \left(B_{i,j} - B_{j,i}\right) \right)_{,j} = 0$$

p(ρ,e)

ρ denotes the average mass density,

u_i, the Favre-averaged velocity

- 3D rectangular geometry
- Fully conservative compressible formulation
- Coupled radiation solver:
- LTE using 4 opacity-distribution-function bins;
- Ray-tracing transport by Feautrier method with 18-ray angular quadrature
- Non-ideal (tabular) EOS
- 4th order Padé spatial discretization
- 4th order Runge-Kutta time integration
- Turbulence models:

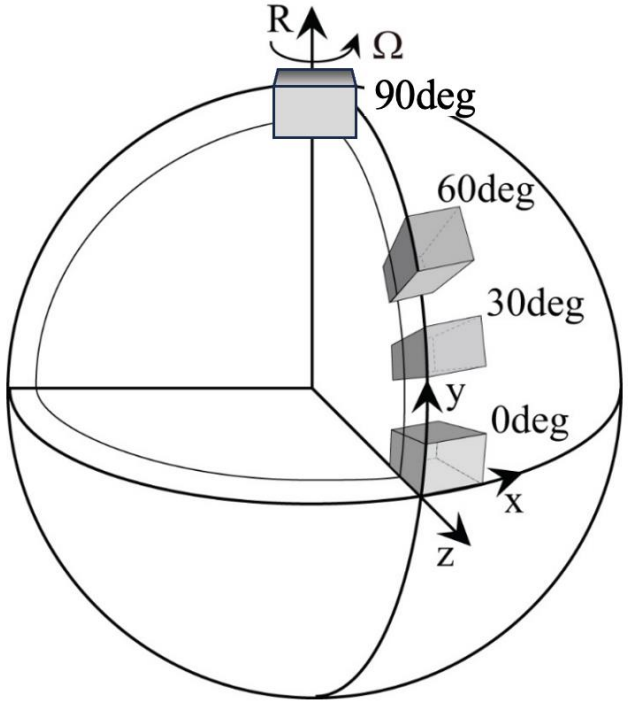
- Compressible Smagorinsky model
- Compressible Dynamic Smagorinsky mode (Germano et al., 1991; Moin et al., 1991)
- MHD subgrid models (Balarac et al., 2010)
- DNS+Hyperviscosity approach

- MPI parallelization

We performed two series of 3D radiative hydrodynamic models:

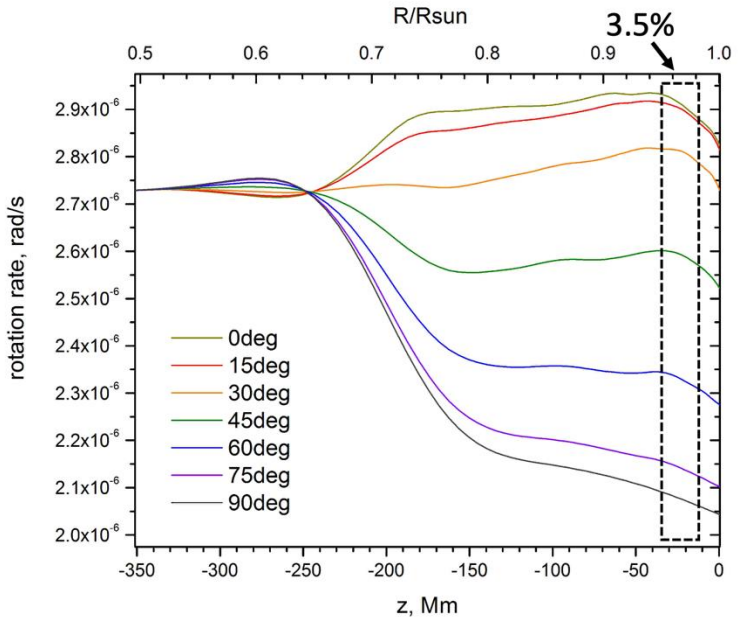
1. For the rotation rate of Prot ~ 27 days at four latitudes.
2. For the realistic rotation rate derived from the global helioseismology measurements during the deep solar minimum in 2008. These computations are performed for the local areas located at different latitudes with 15-degree intervals from the equator to the North Pole.

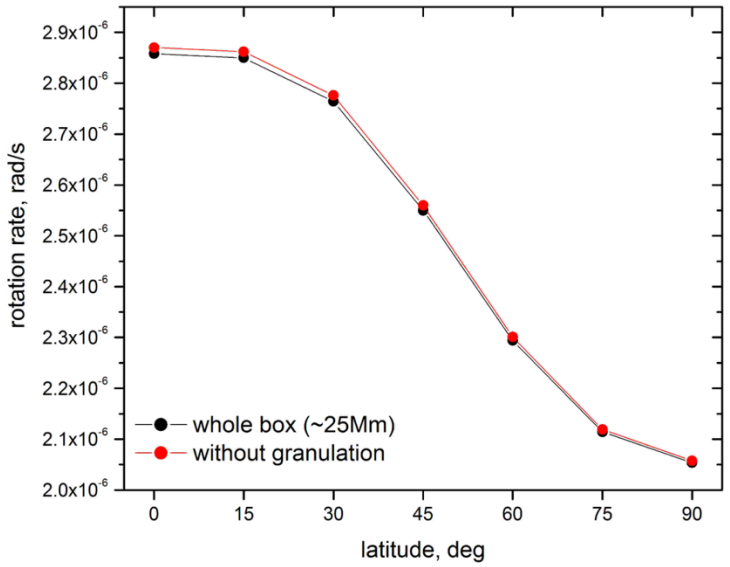
Modeling of the solar rotation in a local computational domain



Scheme of the computation box location relative to the Sun's equator and rotation axis.

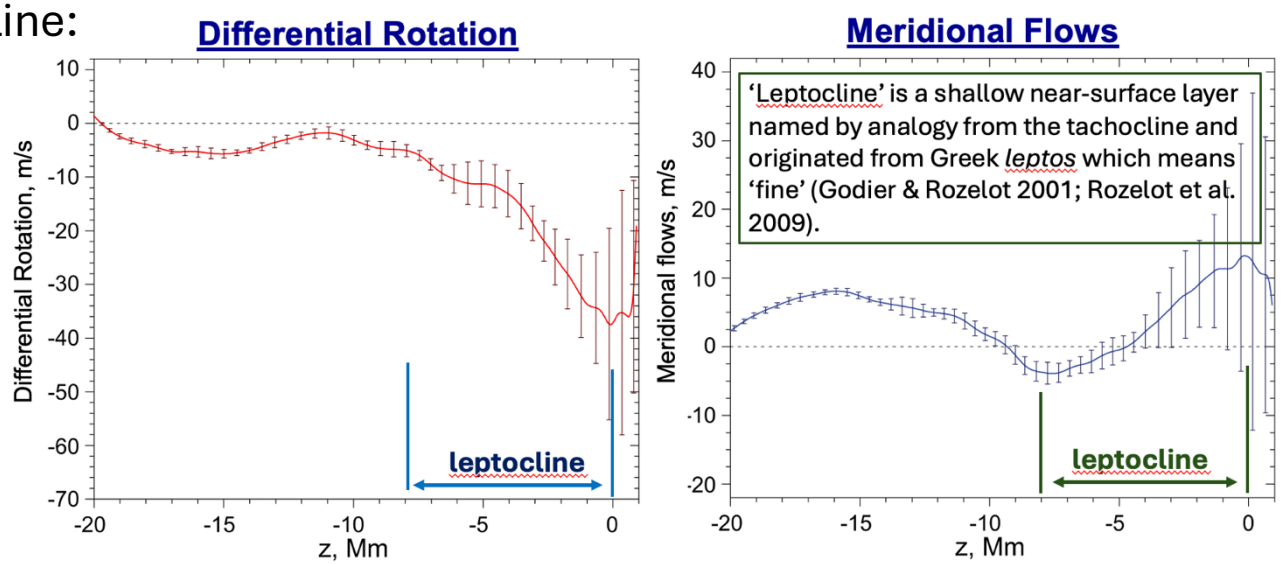
Mean Solar Rotation Rate from SDO/HMI





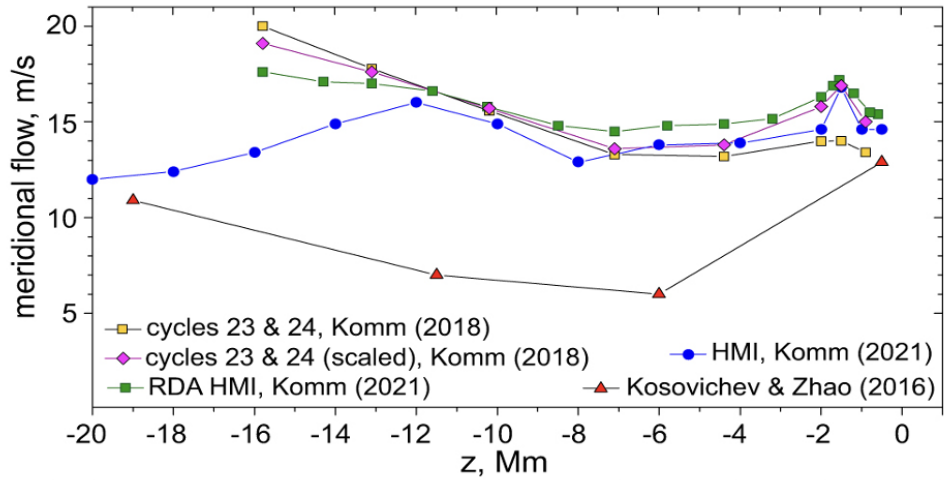
Modeling of the Subsurface Structure of the Sun

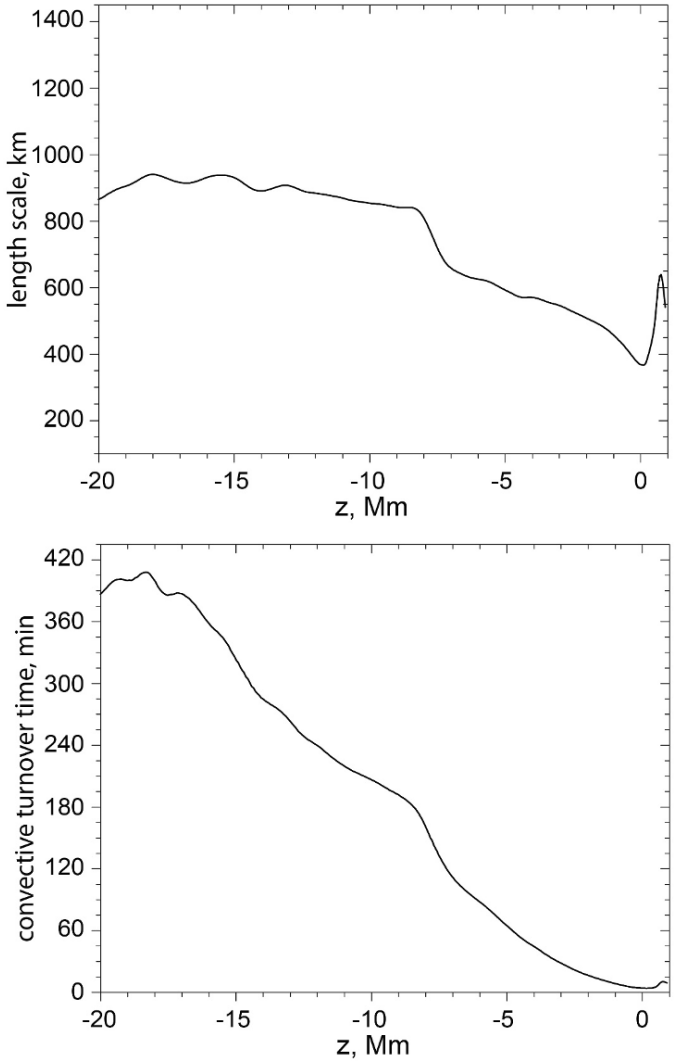
Leptocline:



Mean radial profiles of the azimuthal (rotational) velocity relative to the imposed Carrington rotation rate (left panel) and the meridional flow component of the flow velocity (right panel) at 30 degrees latitude (Kitiashvili et al., 2023). The vertical bars show 1s velocity deviations from the mean values.

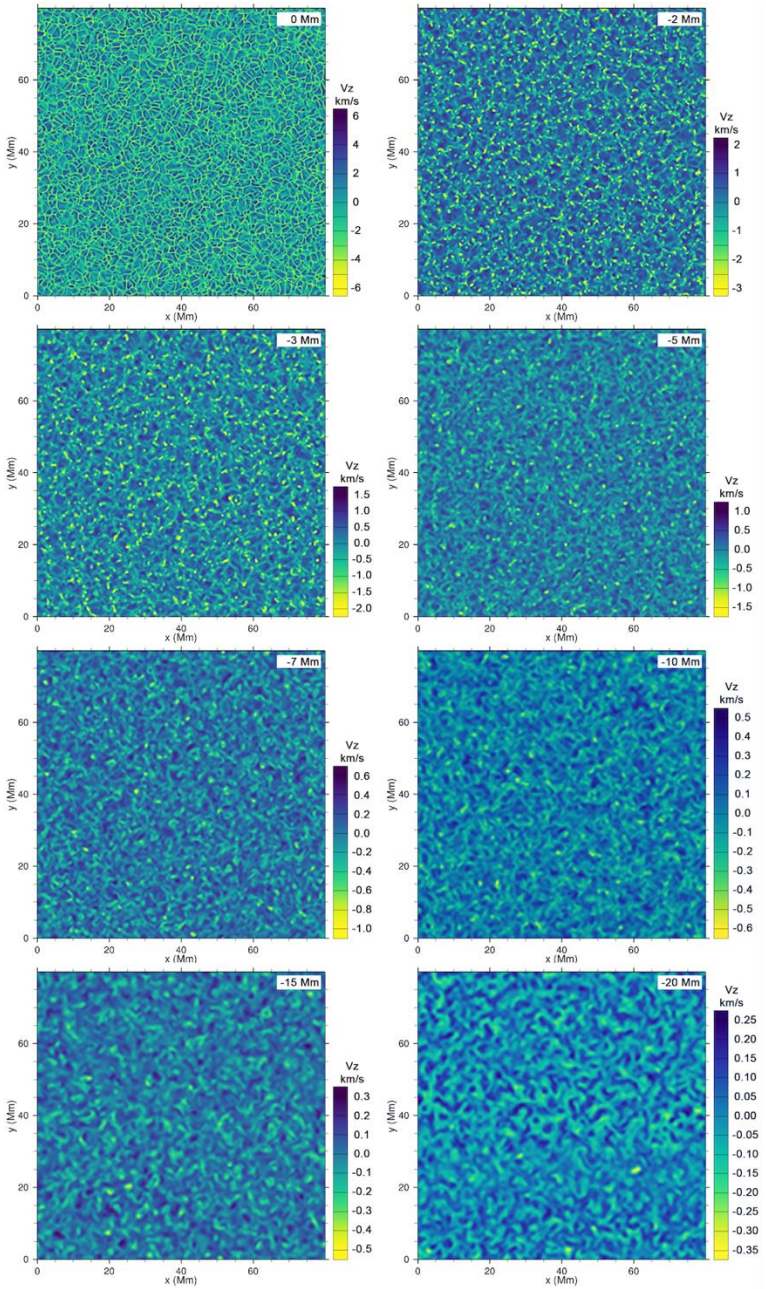
Helioseismic inferences of the meridional circulation at 30 degrees latitude.





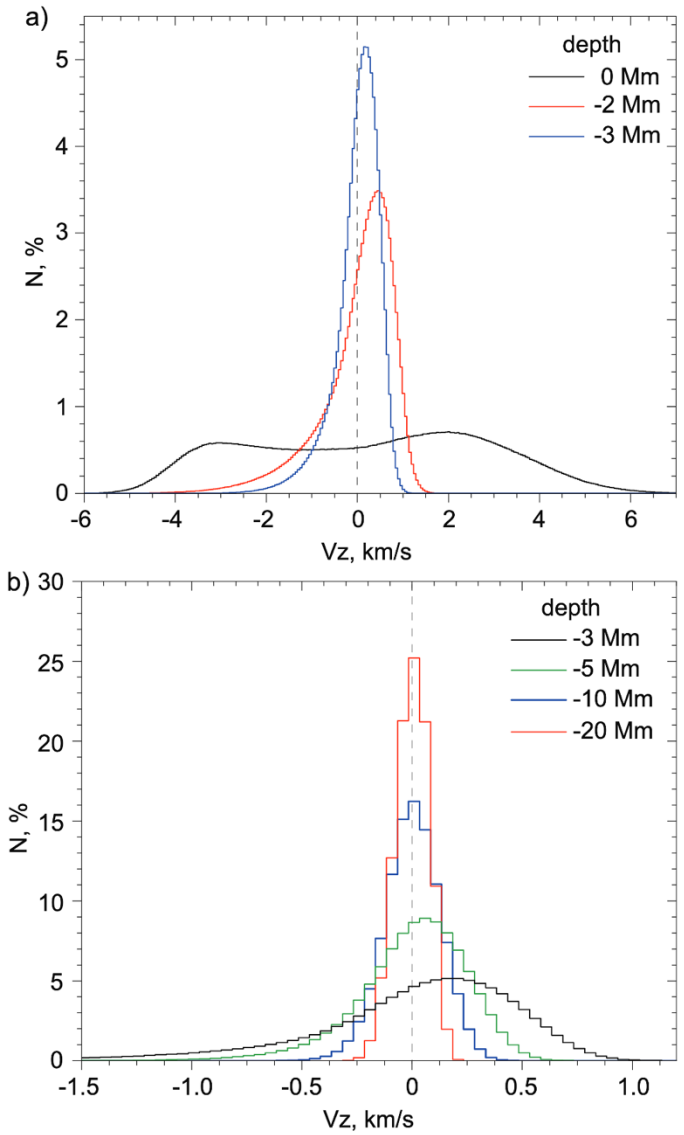
Radial profiles of the characteristic length scale (top panel) and convective turnover time (bottom). A layer approximately 8 Mm in depth corresponds to a fine substructure of the Near-Surface Shear Layer, known as the leptocline (Kitiashvili et al., 2023).

Change in the Turbulent Structure of the Sun in the Upper Layers of the Convection Zone

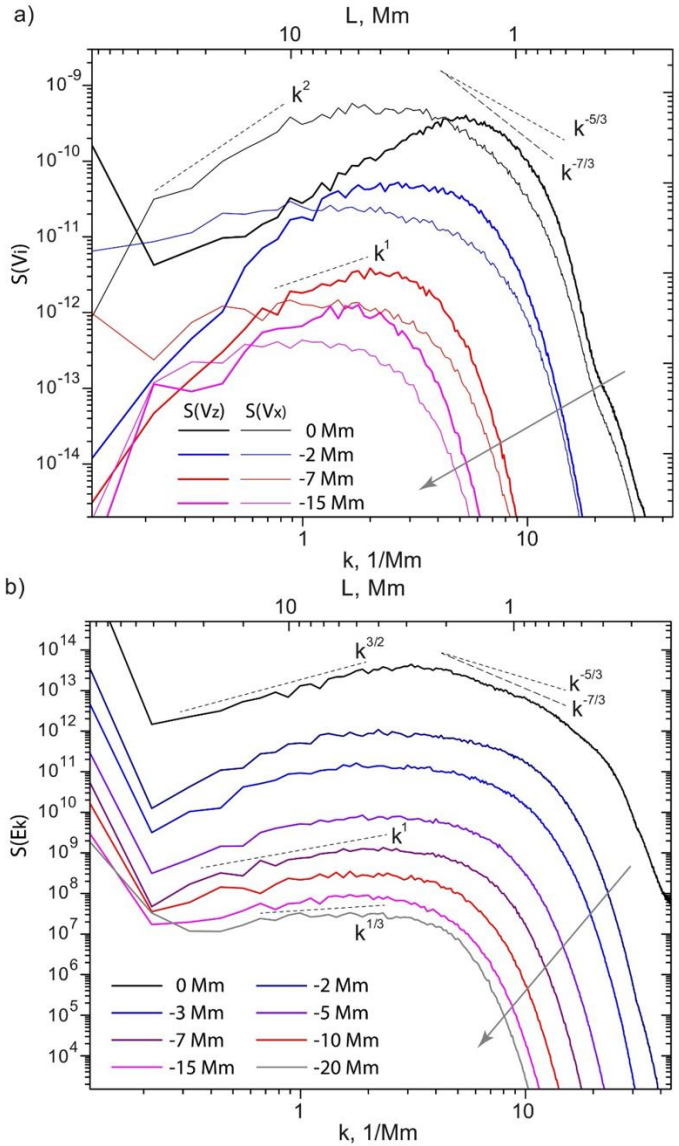


Snapshots of the radial (vertical velocity) from the 3D radiative hydrodynamic model for 8 layers in the solar convection zone at 0 Mm (photosphere), –2 Mm, –3 Mm, –5 Mm, –7 Mm, –10 Mm, –15 Mm, and –20 Mm below the surface, showing qualitative changes of turbulent convection. Brighter colors correspond to the downflows.

The vertical velocity distribution



Turbulent spectra



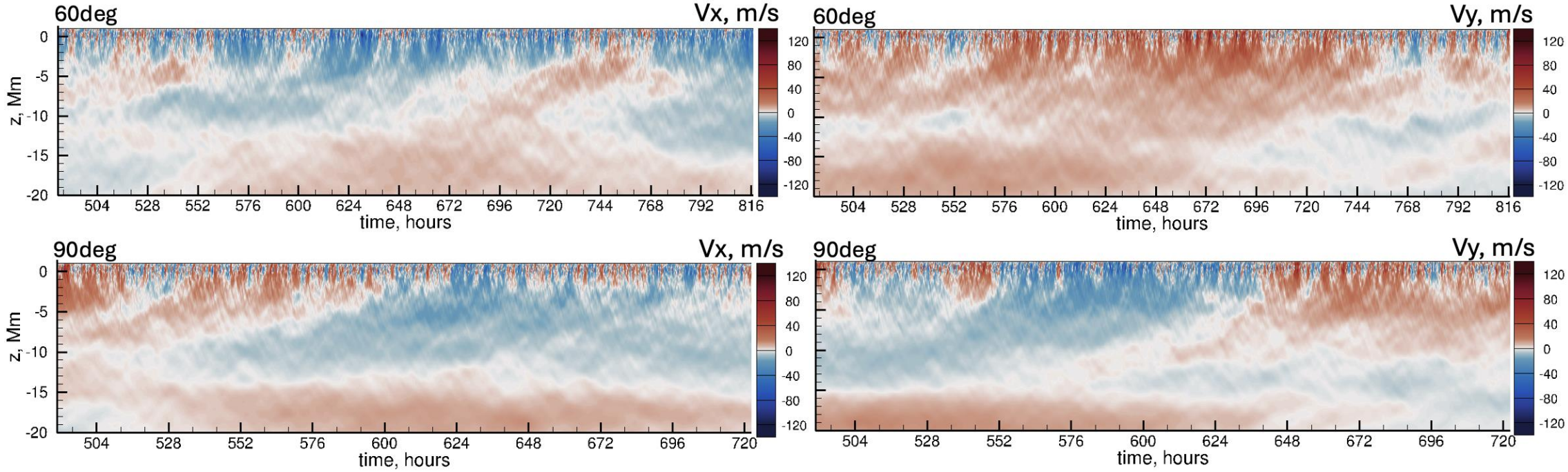
Turbulent spectra of the radial (Vz, thick curves) and azimuthal (Vx, thin curves) components of velocity (panel a) and the kinetic energy density (panel b) at the different depths. The gray arrows indicate the direction from the surface to the interior (Kitiashvili and Wray, 2025).

Modeling of the Polar and High-Latitude Regions

Carrington Rotation Rate:

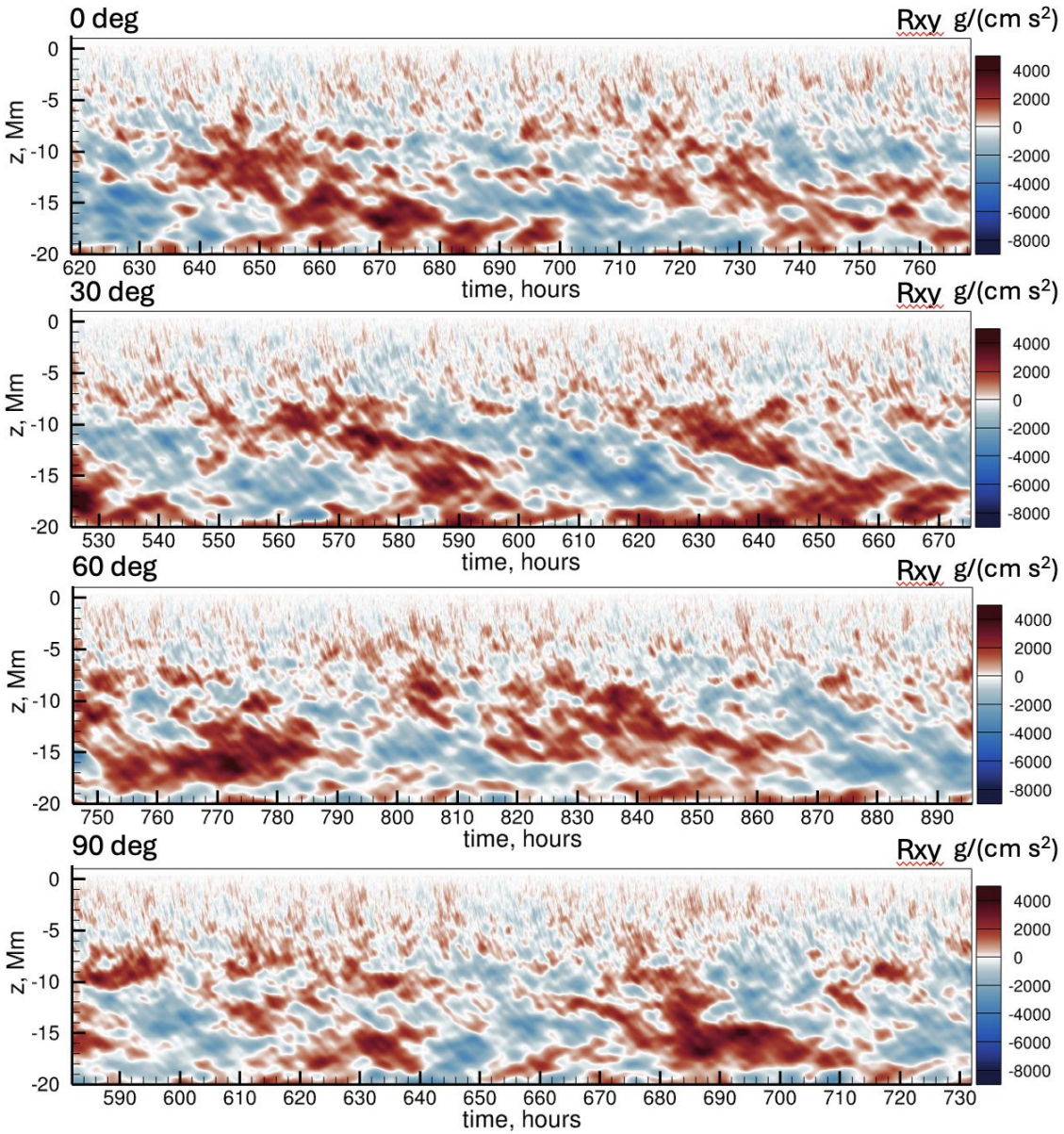
Differential rotation

Meridional flows

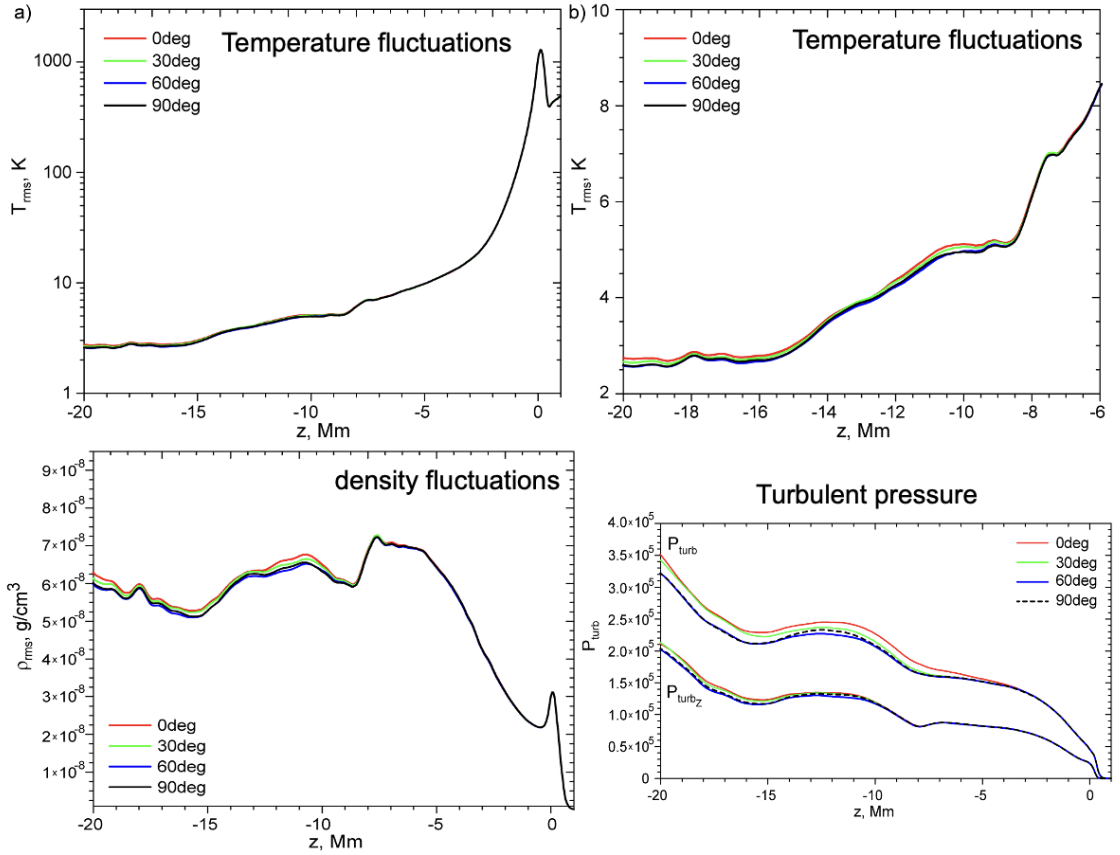


The mean variations of the azimuthal (Vx, left) and meridional (Vy, right) components of velocity as a function of time and depth at high latitudes: 60 and 90 degrees.

Evolution of Reynolds Stresses from Equator to the Northern Pole



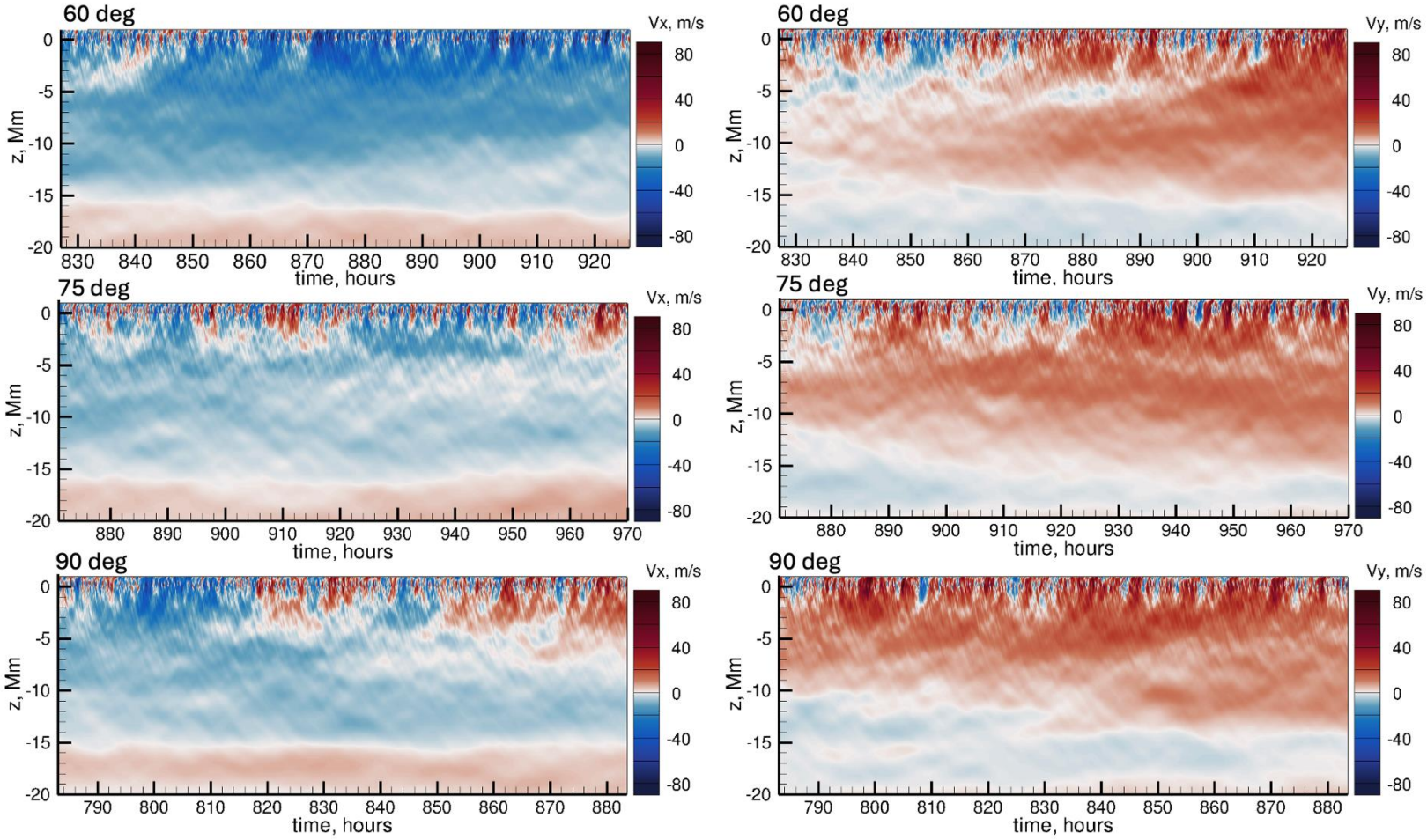
Effect of the Coriolis force on the Thermodynamic Structure of Subsurface Layers



Realistic Rotation Rate:

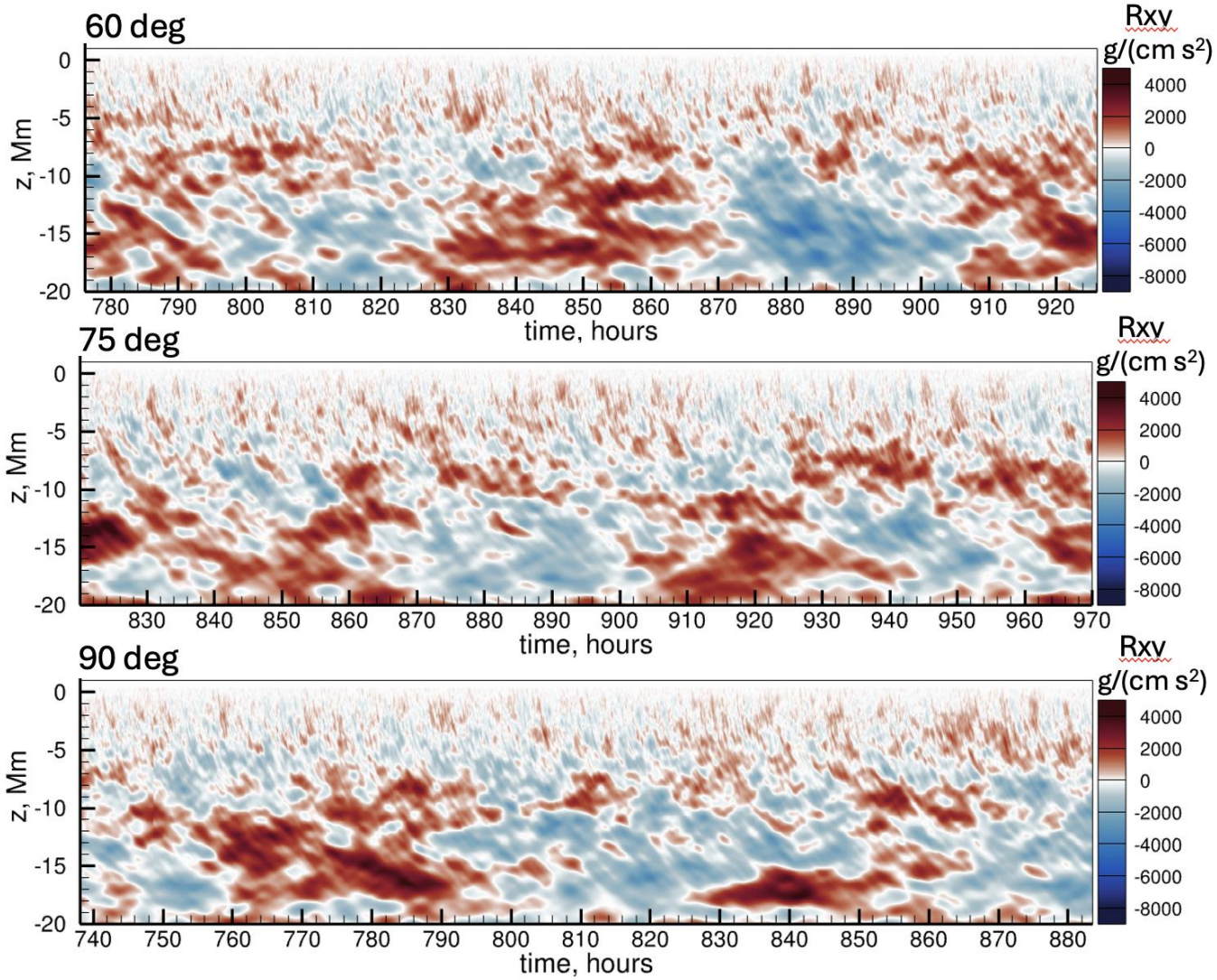
Differential rotation

Meridional flows



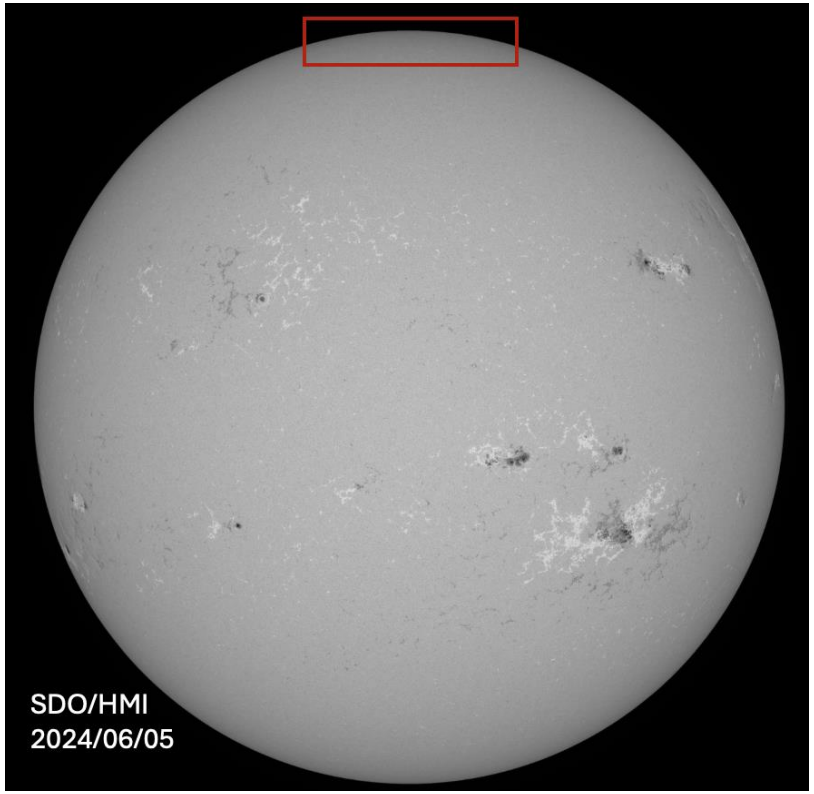
The mean variations of the azimuthal (Vx, left) and meridional (Vy, right) components of velocity as a function of time and depth at three latitudes latitudes: 60, 75, and 90 degrees.

Reynolds Stresses at the high latitudes



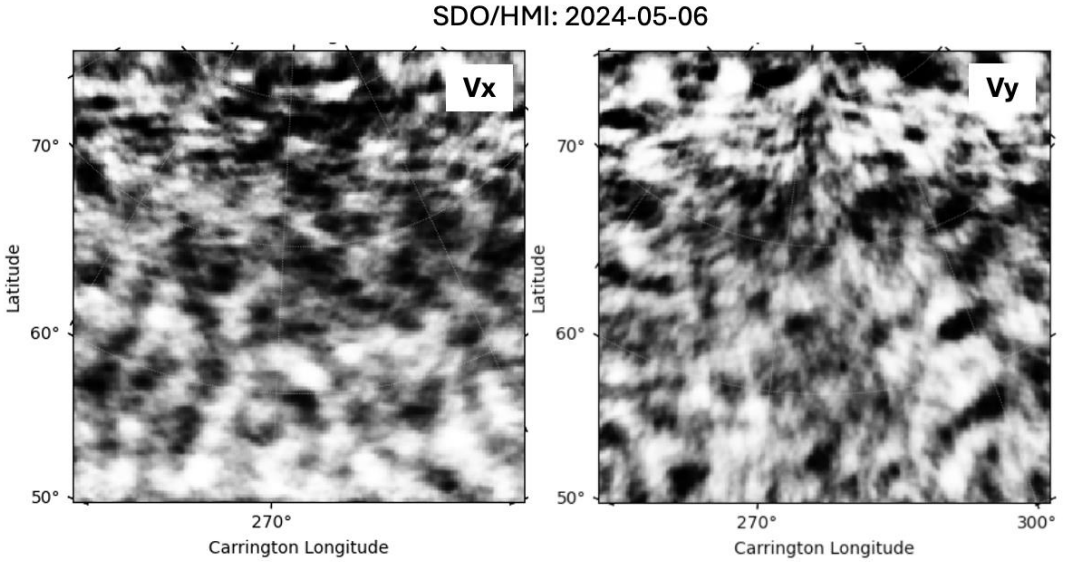
Observations of Solar Polar Regions with SDO/HMI and Hinode/SOT

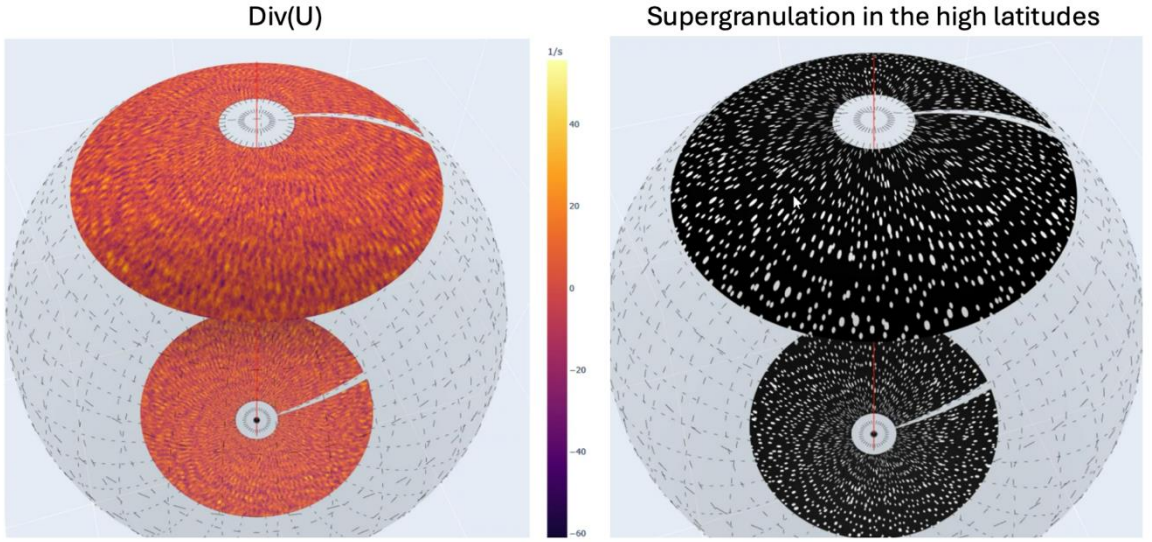
Polar Region Observations with SDO/HMI



Composite image of the continuum intensity and magnetic field from SDO/HMI. The red box indicated a region of interest.

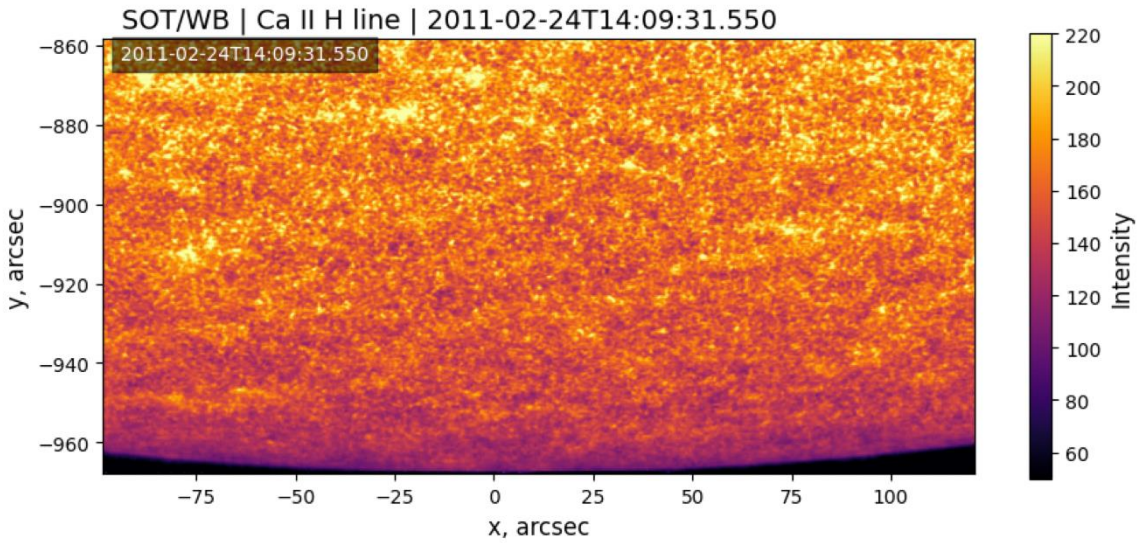
An example of the Vx (left) and Vy (right) velocity maps obtained with the HMI local helioseismology pipeline. The images correspond to the near-surface layer.





Distribution of the flow divergence (left) and identified supergranulation in the vicinity of the North and South poles of the Sun.

Observations of Polar Regions with Hinode/SOT



South pole observation in CaIIH line with Hinode/SOT instrument.

Acknowledgements:
This work is supported by NASA Heliophysics Guest Investigator Program (23-HGIO23-0077), and Science DRIVE (Diversify, Realize, Integrate, Venture, Educate) Center Program (COFFIES Project “Consequences of Fields and Flows in the Interior and Exterior of the Sun”; 80NSSC22M0162). Resources supporting this work were provided by the NASA High-End Computing (HEC) Program through the NASA Advanced Supercomputing (NAS) Division at Ames Research Center.

Conclusions

To investigate the evolution and structure of subsurface convection in the presence of rotation and the underlying physical processes, we performed 3D radiative hydrodynamics simulations, taking into account all essential physics and employing sub-grid scale turbulence models. The simulations revealed the development of radial differential rotation and formation of a shallow ~10 Mm-deep substructure of the Near-Surface Shear Layer – the leptocline – associated with a steep radial gradient of the angular velocity and with changes in the thermodynamic and structural properties of convection at the bottom of the hydrogen ionization zone.

The leptocline constitutes the upper part of the Near-Surface Shear Layer. The interface between the leptocline and deeper layers is characterized by overshooting downdrafts, which may intensify the turbulent mixing below the leptocline layer. The Coriolis force has a noticeable impact on the thermodynamic structure of convection, mainly below the leptocline, where the local Rossby number decreases significantly compared to the near-surface layers of solar convection.

Similar to the case where the Carrington rotation rate is imposed for all latitudes, simulation results with realistic solar rotation rate show the smoother transition from the upper layers of the convection zone (above 8Mm) to the deeper layers, with less prominent signatures of the polar vortical motions.

Finally, we examine the possibility of using SDO/HMI and Hinode/SOT observations of polar regions. The preliminary results allow us to capture supergranular flows at high latitudes using the time-distance helioseismology inferences produced by the SDO/HMI data pipeline. Analysis of Hinode/SOT level-1 data suggests the possibility of high-resolution analysis of surface and subsurface dynamics in the polar regions.